

NEAR-EARTH BINARIES AND TRIPLES: ORIGIN AND EVOLUTION OF SPIN-ORBITAL PROPERTIES

JULIA FANG¹ AND JEAN-LUC MARGOT^{1,2}
Draft version November 9, 2018

ABSTRACT

In the near-Earth asteroid population, binary and triple systems have been discovered with mutual orbits that have significant eccentricities as well as large semi-major axes. All known systems with eccentric orbits and all widely-separated primary-satellite pairs have rapidly rotating satellites. Here we study processes that can elucidate the origin of these spin-orbital properties. Binary formation models based on rotational fissioning can reproduce asynchronous satellites on orbits with high eccentricities and a wide range of separations, but do not match observed properties. We explore whether any evolutionary mechanisms can link the spin and orbital parameters expected from post-fission dynamics to those observed today. We investigate four processes: tidal torques, radiative perturbations (BYORP), close planetary encounters, and Kozai oscillations. We find that a combination of post-fission dynamics and tidal evolution can explain nearly all the spin-orbit properties in a sample of nine well-characterized near-Earth binaries and triples. The other mechanisms may act but are not required to explain the observed data. Lastly, we describe evolutionary pathways between observed spin-orbital states including synchronous and circular, asynchronous and circular, and asynchronous and eccentric configurations.

Subject headings: minor planets, asteroids: general – minor planets, asteroids: individual (2000 DP107, 1999 KW4, 2002 CE26, 2004 DC, 2003 YT1, Didymos, 1991 VH, 2001 SN263, 1994 CC)

1. INTRODUCTION

The study of near-Earth asteroids (NEAs) and main belt asteroids (MBAs) with satellites can yield important information about their fundamental physical properties as well as their formation and evolution (Merline et al. 2002; Pravec et al. 2006). In these multi-component systems, analysis of the relative positions between components can quantify their mutual orbits as well as the total mass of the system. In the near-Earth population, binary and triple asteroids are typically discovered by radar (24 out of 37 as of October 2011) during a close approach to Earth, which can provide detailed physical and orbital information about the system. Studies by Margot et al. (2002) and Pravec et al. (2006) have determined that approximately 15% of NEAs larger than 200 meters in diameter have satellites. Due to the d^{-4} dependence in the return signal (where d is the distance to the target), radar observations have not identified MBA systems so far. Small MBA systems have generally been discovered through light curve observations whereas larger MBA systems have typically been discovered with adaptive optics observations.

Orbital solutions of NEA systems indicate that some of their satellites possess unexplained spin-orbital properties including asynchronous³ rotation, eccentric orbits,

and wide separations from their primaries. All known satellites with semi-major axes larger than 7 primary radii are asynchronously rotating and all known satellites with eccentricities greater than 0.05 are asynchronously rotating, suggesting that these properties have a common origin. Accordingly, we seek an explanation for these observed spin-orbital characteristics by examining if any evolutionary processes can lead to the observed data.

Previous attempts to investigate the observed properties of NEA systems include tidal evolution as a mechanism for eccentricity excitation or de-excitation (Taylor & Margot 2011, and references therein). Other studies have described the orbital evolution of small binary asteroids by the binary YORP (BYORP) effect (Ćuk & Burns 2005; Ćuk 2007). BYORP is caused by the asymmetric re-radiation of light by an irregularly shaped secondary in synchronous rotation with its primary, and this effect can cause orbital migration and an increase or decrease of the mutual orbit's eccentricity (Goldreich & Sari 2009; Ćuk & Nesvorný 2010; McMahon & Scheeres 2010a,c; Steinberg & Sari 2011). An alternative process to modify an orbit's semi-major axis and eccentricity is through close scattering encounters by terrestrial planets, as described in a companion paper by Fang & Margot (2011) for binaries and by Fang et al. (2011) for triple systems. Another possibility is that NEA binaries can have their eccentricities excited through Kozai oscillations (Kozai 1962).

In this paper, we examine all of these proposed evolutionary processes to find a coherent model that can explain the observed spin-orbital characteristics of satel-

¹ Department of Physics and Astronomy, University of California, Los Angeles, CA 90095, USA

² Department of Earth and Space Sciences, University of California, Los Angeles, CA 90095, USA

³ In this paper, binaries with an absence of spin-orbit synchronization are called *asynchronous binaries*. Binaries with a secondary spin period synchronized to the mutual orbit period are called *synchronous binaries*. Binaries with both primary and secondary spin periods synchronized to the mutual orbit period are called *doubly synchronous binaries*. Most NEA binaries are *synchronous*. Note that our terminology is different from that of Pravec & Harris

(2007), who use the term “asynchronous binaries” for binaries with spin-orbit synchronization. If generalization to systems with more than one satellite is needed, we affix the terms *synchronous* and *asynchronous* to the satellites being considered.

Table 1
Well-Characterized Near-Earth Binaries and Triples

System	R_p (km)	M_p (kg)	R_s (km)	M_s (kg)	a (km)	e	a/R_p	CA Distance (AU)	MOID (AU)
(185851) 2000 DP107 ^a	0.40	4.38×10^{11}	0.150	2.19×10^{10}	2.62 ± 0.162	$0.01_{-0.01}^{+0.015}$	6.6	0.058 in 2008	0.015
(66391) 1999 KW4 ^b	0.66	2.35×10^{12}	0.226	1.35×10^{11}	$2.55_{-0.01}^{+0.03}$	$0.008_{-0.008}^{+0.012}$	3.9	0.089 in 2002	0.013
(276049) 2002 CE26 ^c	1.75	2.17×10^{13}	0.150	1.37×10^{10}	$4.87_{-0.12}^{+0.28}$	$0.025_{-0.006}^{+0.008}$	2.8	0.102 in 2004	0.100
*2004 DC ^d	0.17	3.57×10^{10}	0.030	1.96×10^8	$0.75_{-0.05}^{+0.04}$	$0.30_{-0.04}^{+0.07}$	4.4	0.026 in 2006	0.009
*(164121) 2003 YT1 ^e	0.55	1.89×10^{12}	0.105	1.32×10^{10}	$3.93_{-0.13}^{+1.47}$	$0.18_{-0.01}^{+0.02}$	7.1	0.073 in 2004	0.002
(65803) Didymos ^f	0.40	5.24×10^{11}	0.075	3.45×10^9	$1.18_{-0.02}^{+0.04}$	$0.04_{-0.04}^{+0.05}$	3.0	0.048 in 2003	0.04
*(35107) 1991 VH ^g	0.60	1.40×10^{12}	0.240	8.93×10^{10}	$3.26_{-0.04}^{+0.03}$	0.06 ± 0.02	5.4	0.046 in 2008	0.026
(153591) 2001 SN263 #1 ^h	1.30	9.17×10^{12}	0.230	9.77×10^{10}	$3.80_{-0.02}^{+0.01}$	$0.016_{-0}^{+0.005}$	2.9	0.066 in 2008	0.049
*(153591) 2001 SN263 #2 ^h	1.30	9.17×10^{12}	0.530	2.40×10^{11}	$16.63_{-0.38}^{+0.39}$	$0.015_{-0.010}^{+0.022}$	13	0.066 in 2008	0.049
(136617) 1994 CC #1 ⁱ	0.31	2.59×10^{11}	0.057	5.80×10^9	1.73 ± 0.02	$0.002_{-0.002}^{+0.009}$	5.6	0.017 in 2009	0.016
*(136617) 1994 CC #2 ⁱ	0.31	2.59×10^{11}	0.040	9.10×10^8	$6.13_{-0.12}^{+0.07}$	$0.19_{-0.022}^{+0.015}$	20	0.017 in 2009	0.016

Well-characterized NEA binaries and triples as defined in this paper have some known physical and orbital properties: approximate component sizes (primary radius R_p , secondary radius R_s), masses (primary mass M_p , secondary mass M_s), semi-major axis a , and eccentricity e . Known asynchronous satellites are marked with a *. This table shows nominal values adopted for this study as well as plausible $1-\sigma$ uncertainties for a and e . Uncertainties for sizes are roughly $\sim 20\%$ and for masses are roughly $\sim 10\%$. Methods for obtaining parameters and uncertainties are described in the text (Section 1.1). Also shown here is close approach (CA; $\lesssim 0.1$ AU) data, including the most recent approach at the time of radar observation and the current MOID (see text) with Earth, given by the JPL Small-Body Database. For the triple systems, 2001 SN263 and 1994 CC, we list the inner satellite first and the outer satellite second.

^aMargot et al. (2002)

^bOstro et al. (2006)

^cShepard et al. (2006)

^dTaylor et al. (2008)

^eNolan et al. (2004)

^fBenner et al. (2010)

^gMargot et al. (2008); Pravec et al. (2006)

^hNolan et al. (2008); Fang et al. (2011)

ⁱBrozovic et al. (2011), Fang et al. (2011)

lites in NEA systems. In the remainder of this section, the current population of well-characterized NEA binaries and triples is presented in Section 1.1, relevant lifetimes are defined in Section 1.2, and binary and triple formation is introduced in Section 1.3. Then, we examine each main evolutionary process in turn: Section 2 discusses tidal evolution timescales and critical semi-major axes pertinent for satellite spin synchronization, Section 3 summarizes current theories on BYORP evolution and their applicability, Section 4 evaluates if planetary encounters can explain the eccentric and wide orbits of asynchronous satellites, and Section 5 discusses Kozai resonance and its timescales. We find that tidal evolution can explain the observed spin-orbital characteristics of nearly all NEA systems, and we discuss possible evolutionary pathways between observed spin-orbital states in Section 6. We summarize this study and its implications in Section 7.

1.1. Sample of Well-Characterized Binaries and Triples

We compile a sample of well-characterized NEA systems (Table 1) that consists of 7 binaries and 2 triples. We will refer to this sample throughout this paper as we study the spin-orbital origin of these systems. This sample includes all NEA systems with known estimates of system mass, semi-major axis, eccentricity, and component sizes. In practice, only systems observed with radar fall in this class.

Primary and secondary sizes of these NEAs are obtained from radar shape modeling (when available), or from range extents estimated from radar images. System

masses are derived from orbital solutions, which are computed based on measurements of range and Doppler separations. For triple systems, individual mass estimates are obtained through dynamical 3-body orbital fits. For some binaries, the masses of the primary and of the secondary have been directly estimated from the observed reflex motion. For all others, the system mass is apportioned to the individual components by using size ratios and a common density assumption.

The semi-major axes and eccentricities of these well-characterized NEAs are obtained through orbital fits to radar astrometry, and we list them in Table 1 and plot them in Figure 1. Brozovic et al. (2011) have reported a list of asynchronous satellites that are rapidly rotating, which includes the following satellites in our sample of NEA systems: 2003 YT1, 1991 VH, 2004 DC, and the outer satellites of 2001 SN263 and 1994 CC. These asynchronous satellites are marked with asterisks in the first column of Table 1 and represented by unfilled circles in Figure 1. In this sample, asynchronous rotators include all satellites with adopted eccentricities greater than 0.05 and all satellites with semi-major axes greater than 7 primary radii. These correlated spin-orbital properties are likely due to the decreasing effects of tidal dissipation (which can synchronize the satellite’s spin to its orbital period and circularize orbits) at larger semi-major axes. The exploration of evolutionary processes that can explain these spin-orbital characteristics will be discussed in the bulk of this paper.

Plausible $1-\sigma$ uncertainties for semi-major axes and eccentricities are compiled from published values (when

available) and listed in Table 1 along with the adopted values. When published uncertainties are not available, we obtain uncertainties by determining their $1-\sigma$ confidence levels (e.g. Cash 1976; Press et al. 1992). For each considered parameter, we hold it fixed at a range of values while simultaneously fitting for all other parameters. Since only one parameter is held fixed at a time, a $1-\sigma$ confidence region is prescribed by the range of solutions which exhibit chi-square values within 1.0 of the best-fit chi-square.

All of these well-characterized NEA systems are observed by radar and have varying degrees of observational coverage and quality. We have high confidence in the datasets for binaries 1999 KW4, 2000 DP107, and 1991 VH as well as triples 2001 SN263 and 1994 CC. These systems have extensive, high signal-to-noise measurements on ~ 10 epochs over ~ 2 weeks, or have been observed on 2 separate apparitions. We have moderate confidence for 2002 CE26, Didymos, 2004 DC, and 2003 YT1, which all have ~ 50 – 150 measurements over 4–14 days. These high and moderate confidence datasets comprise the well-characterized sample of NEA binaries and triples listed in Table 1. We also mention another radar-observed binary designated 1998 ST27 with an asynchronously rotating satellite (Benner et al. 2003) due to its uniquely large separation. 1998 ST27 has a low confidence dataset with fewer than 40 measurements and inconsistencies in orbit solutions, and thus we can only determine a lower bound on its semi-major axis of $\gtrsim 12$ primary radii or $\gtrsim 5$ km. Its actual semi-major axis may be much higher. Its large separation makes 1998 ST27 the widest NEA binary discovered so far.

Since all of these NEA systems in Table 1 are characterized by radar data, this sample is biased towards binaries and triples discovered through radar techniques, which typically require close approaches with Earth of $\lesssim 0.1$ AU. Close approach data, including the most recent approach near the time of radar observations and the current minimum orbital intersection distance (MOID) with Earth, are listed in Table 1. The MOID describes the minimum distance between two elliptical orbits and disregards the positions of the bodies in their orbits (Sitarski 1968), and is valid as long as the osculating orbital elements approximate the actual orbits. These orbital elements certainly change over long periods of time and therefore close approaches to Earth less than the current MOID could have occurred in the past.

1.2. Dynamical and Collisional Lifetimes

NEAs are short-lived and have dynamical lifetimes on the order of a few million years (Bottke et al. 2002). These average lifetimes represent how long they can survive in near-Earth space before plunging into the Sun, getting ejected from the Solar System, or colliding into a planet. Due to these short NEA lifetimes, the near-Earth population is continually replenished by small ($\lesssim 10$ km) MBAs. These small MBAs migrate into near-Earth space through unstable main belt regions that are permeated by strong resonances with Jupiter and Saturn. Resonance capture is enabled by radiation forces and collisions, which bring MBAs into these unstable main belt regions. While in the main belt, these asteroids have collisional lifetimes that are dependent on their sizes. For example, an asteroid 500 meters in radius will have a col-

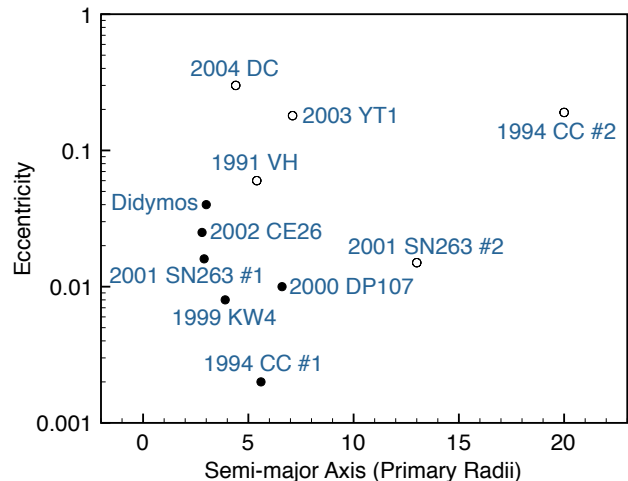


Figure 1. This plot shows the well-characterized NEA systems in eccentricity and semi-major axis (in primary radius) space, whose orbital parameters are taken from Table 1. Asynchronous satellites are represented by unfilled circles and synchronous satellites are marked with filled circles.

lisional lifetime of $\sim 3.8 \times 10^8$ years (Bottke et al. 2005).

Clearly, collisional lifetimes (while in the main belt) are much greater than dynamical lifetimes (while in near-Earth space). It is quite plausible that many observed NEA systems had their satellites formed while still in the main belt, and so their total lifetimes as a binary or triple will be dominated by their prior collisional lifetime. An important implication of binary/triple formation in the main belt is that some evolutionary processes have a longer period of time within which they may occur. The examination of these evolutionary processes constitute the bulk of this paper.

1.3. Binary and Triple Formation

Binary and triple asteroids form through the generally accepted rotational fission model (Margot et al. 2002; Pravec et al. 2006; Walsh et al. 2008). The likely spin-up mechanism is the thermal YORP effect (Rubincam 2000), which causes mass shedding from the primary. In this subsection, we introduce the post-fission dynamics model of Jacobson & Scheeres (2011), and in particular we evaluate its relevance in explaining any of the observed spin-orbital characteristics of NEA binaries and triples.

Jacobson & Scheeres (2011) describe the immediate ($\lesssim 1000$ years) dynamics following rotational fission, which include YORP (to spin up the initial body, and this is the only time a non-gravitational force is incorporated in their model), secondary fission (a satellite is rotationally accelerated and then fissions to create another satellite), tri-axial gravitational potentials, tides, and solar gravitational perturbations. The immediate result after initial fissioning of the primary is a chaotic binary, and subsequent evolutionary processes are mainly determined by mass ratio (mass of secondary/mass of primary).

Binaries with high mass ratios (> 0.2) do not undergo secondary fission and instead experience tidal dissipation to become doubly synchronous. This may lead to

a contact binary state if BYORP contracts the orbit. Low mass ratio binaries will mostly disrupt unless they are allowed to experience secondary fission, which creates an initially chaotic triple system. The chaotic triple can stabilize and become a binary by ejection or collision of a satellite, which can lower the system’s angular momentum and energy. Resulting binaries that are stable after 1000 years of evolution are shown in Figure 2 (Jacobson & Scheeres 2011).

In Figure 2, we point out two scenarios of interest. First, early tidal evolution can lead to a commonly observed type of binary: a synchronous satellite with a separation of ~ 4 primary radii and an eccentricity of ~ 0.3 – 0.4 that will continue to damp by tides. Second, some satellites have large separations (up to ~ 10 – 16 primary radii) from their primary with correspondingly large eccentricities (up to ~ 0.6 – 0.8). These wide primary-satellite pairs may explain observed satellites located at large semi-major axes, although the eccentricities predicted by the post-fission dynamics model are larger than any observed value.

Triple formation can occur through secondary fission or another round of YORP-induced primary fission. Jacobson & Scheeres (2011) include secondary fission in this model and their simulations produce no stable triple systems after 1000 years of evolution. They do not model additional rounds of YORP-induced primary fission, which remains a plausible explanation for the formation of triple systems. We add the hypothesis that triples form by first creating a wide binary (such as those seen in post-fission simulations) through primary fission, and then a closer-in satellite is formed during a subsequent round of primary fission. This possibility is also supported by observations of wide binary 1998 ST27 that has a separation ($\gtrsim 12$ primary radii) consistent with the outer satellite’s separation (~ 13 primary radii) in triple 2001 SN263.

Other studies discussing spin-up fissioning either do not mention or only provide scant information about the resulting spin-orbital parameters of a newly-formed satellite (e.g. Scheeres 2007; Holsapple 2010; Walsh et al. 2008). The fissioning model of Walsh et al. (2008) does not attempt to simulate post-fission dynamics and so does not include tidal interactions. In their simulations, when satellites grow to 0.3 primary radii, their separations are 2 – 4.5 primary radii and their eccentricities are < 0.15 . This range of eccentricities is lower than that found by Jacobson & Scheeres (2011) and shown in Figure 2.

In essence, the immediate ($\lesssim 1000$ years) dynamics ensuing from this formation scenario provide a pathway for the creation of wide binaries such as 1998 ST27 and potentially the outer satellites in triple systems. However, the eccentricities from post-fission dynamics are too high compared to observed eccentricities, and some of the simulated binaries have small semi-major axes of ~ 2 primary radii that are smaller than any observed separation. Moreover, the spin states of just-formed satellites will be asynchronous. Clearly, if multiple systems are formed by rotational fission and follow the post-fission dynamics model of Jacobson & Scheeres (2011), there will be additional processes that evolve the systems, and the exploration of these processes constitute the bulk and re-

mainder of this paper.

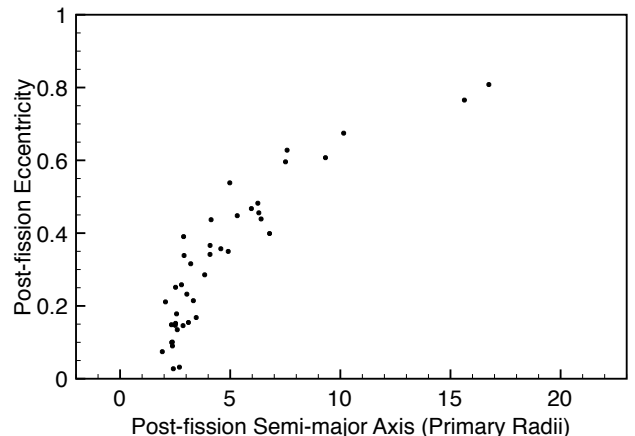


Figure 2. Results from post-fission simulations by Jacobson & Scheeres (2011) are shown after 1000 years of evolution (Seth Jacobson, personal communication, 2011).

2. TIDAL EVOLUTION

In this section, we investigate evolutionary processes due to tidal effects, and whether tides can explain the observed spin-orbital characteristics of satellites in NEA systems. The fastest tidal evolution process (in the absence of other spin-modifying forces) is the synchronization of a satellite’s spin to its orbital period due to the tides raised on the secondary by the primary (Goldreich 1963; Goldreich & Sari 2009). After synchronization, tidal evolution continues by modifying the semi-major axis and eccentricity of the mutual orbit. It is a competing process between the opposing effects of tides raised on a primary (which increase both the semi-major axis and eccentricity) and those raised on the secondary (which cause negligible changes in the semi-major axis, but decrease eccentricity). Tidal evolution ends after the orbit has circularized and the primary’s spin has synchronized to the mutual orbit period, resulting in a doubly synchronous system.

Models of tidal evolution for asteroids are governed by two dimensionless parameters: the effective rigidity $\tilde{\mu}$ and the tidal dissipation factor Q . The non-dimensional effective rigidity $\tilde{\mu}$ is a function of the body’s internal properties such as density ρ and radius R , and is defined as follows for a monolith: $\tilde{\mu} = (19\mu)/(2g\rho R)$ where g represents self-gravity and μ is the body’s rigidity or shear modulus with units of pressure (Murray & Dermott 1999). The effective rigidity is related to the tidal Love number k , where $k = 1.5/(1+\tilde{\mu})$ for a homogeneous solid body. The tidal dissipation factor Q is a quality factor defined as $Q = (2\pi E_0)/(\Delta E)$, which describes the body’s effectiveness at dissipating energy (Murray & Dermott 1999). If we consider the body’s response to tidal oscillations as a harmonic oscillator, E_0 represents the peak energy stored during a cycle and ΔE is the energy dissipated over a cycle. Unfortunately, for small asteroids there are substantial uncertainties in crucial parameters $\tilde{\mu}$ (or k) and Q , in addition to other poorly known effects, such as the frequency de-

pendence of these two quantities, their applicability to porous bodies, or even our ability to capture tidal processes with two idealized numbers.

2.1. Eccentricity Evolution

Post-fission eccentricities (Section 1.3) are significantly higher than observed eccentricities for some NEA systems, and so here we explore the effects of tides in modifying eccentricity. Several models have been considered to facilitate calculations of tidal evolution in asteroids.

In the *monolith* model, asteroids are idealized as uniform bodies with no voids. In this idealization, the effective rigidity $\tilde{\mu}_{\text{mono}}$ is inversely proportional to the square of the asteroid’s radius R : $\tilde{\mu}_{\text{mono}} \propto R^{-2}$ or $k_{\text{mono}} \propto R^2$. To arrive at numerical values, Goldreich & Sari (2009) used the Moon’s radius and Love number k of ~ 0.025 (Williams et al. 2008) and obtained $\tilde{\mu}_{\text{mono}} \sim 2 \times 10^8$ (1 km/ R)². The monolith tidal model has been used to estimate the relative strengths of the components in the Kalliope-Linus binary system. Since its mutual orbit is found to be near-circular, comparison of the relative rates of eccentricity excitation and damping constrains the relative values of $\tilde{\mu}Q$ for the primary and secondary: Margot & Brown (2003) found that $\tilde{\mu}Q$ for the secondary is smaller than that of the primary.

In the *rubble pile* model, asteroids are idealized as gravitational aggregates, i.e. composed of smaller elements held together by gravity only. This assumption is motivated by the low observed densities of NEA systems and the observed “spin barrier” (Pravec et al. 2002). We will consider two separate rubble pile models.

Goldreich & Sari (2009) propose that the relationship between a rubble pile’s effective rigidity $\tilde{\mu}_{\text{rubble}}$ and a monolith’s effective rigidity $\tilde{\mu}_{\text{mono}}$ of comparable composition and size is simply $\tilde{\mu}_{\text{rubble}} \sim 10\sqrt{\tilde{\mu}_{\text{mono}}}$. Thus, this model (Goldreich & Sari 2009) defines a rubble pile’s effective rigidity as $\tilde{\mu}_{\text{rubble}} \sim 10^5\sqrt{2}$ (1 km/ R) or Love number $k_{\text{rubble}} \sim 10^{-5}$ ($R/1$ km). If we assume a common density and tidal quality Q factor between the primary and secondary, the rubble pile model adopted by Goldreich & Sari (2009) gives the ratio of the rates of eccentricity excitation to damping as 19/28 (irrespective of component sizes) for a system with a synchronized secondary. Therefore, in this model the eccentricity will likely damp for such systems. In cases where there are density or Q differences between the components, it is possible the eccentricity can grow.

Jacobson & Scheeres (2011b) find that the Goldreich & Sari (2009) model agrees reasonably well for data of binaries with primary radii of ~ 2 km, but not for systems with very small primary radii. This discrepancy can be resolved using a different Love number dependence on size, and Jacobson & Scheeres (2011b) describe a power law fit to the logarithmic data of known synchronous binaries compiled by Pravec et al. (2006). They find that $\tilde{\mu}_{\text{rubble}} \sim 6 \times 10^4$ ($R/1$ km) or $k_{\text{rubble}} \sim 2.5 \times 10^{-5}$ (1 km/ R). Thus, if we apply this model for binary components of common density and tidal quality factor Q , we find that the ratio of the rates of eccentricity excitation to damping is $(19R_s^2)/(28R_p^2)$, where R_p is the radius of the primary and R_s is the radius of the secondary. Thus, eccentricity will also likely damp in this model.

For all models, the eccentricity evolution for a synchronous satellite’s orbit (Goldreich 1963; Goldreich & Sari 2009) is

$$\frac{de}{dt} = \frac{57}{8} \frac{k_p}{Q_p} \frac{M_s}{M_p} \left(\frac{R_p}{a}\right)^5 ne - \frac{21}{2} \frac{k_s}{Q_s} \frac{M_p}{M_s} \left(\frac{R_s}{a}\right)^5 ne \quad (1)$$

where there are two competing terms corresponding to eccentricity excitation and damping, respectively. This equation is a function of tidal Love number k , tidal quality factor Q , mass M , radius R , semi-major axis a , mean motion n , and eccentricity e . The subscripts p and s represent the primary and secondary, respectively.

Using Equation 1, we calculate the circularization timescales τ_{damp} of all orbits in our NEA sample given their current orbital and physical parameters (Table 1). These timescales are presented in Table 2. In our calculations, we use an assumption of $Q \sim 10-10^2$, which is reasonable for small rocky bodies. We calculate τ_{damp} according to both rubble pile models: the $k \propto R$ model of Goldreich & Sari (2009) and the $k \propto R^{-1}$ model of Jacobson & Scheeres (2011b). With these assumptions, we obtain τ_{damp} by calculating the $1/e$ damping timescale (here e is Euler’s constant) for eccentricity by numerically integrating Equation 1.

For the cases of 1999 KW4, 2001 SN263 #1, 1994 CC #1, and 1994 CC #2, the tidal Love number model of Goldreich & Sari (2009) gives a larger de/dt for the excitation term than for the damping term (which occurs for these cases due to density differences between the primary and satellite), and so their eccentricities would theoretically be predicted to increase. However, most of these satellites are observed to have circular orbits, which indicates that either the densities are incorrect, there are Q differences between the primary and satellite, and/or the tidal model is incorrect. For these cases, we suspect that the satellite densities are in error. If we assume that all components have a density equal to that of the primary when we compute de/dt , then we find that their eccentricities will damp as predicted by theory.

The eccentricity damping timescales calculated from Equation 1 and presented in Table 2 show that there are differences of several orders of magnitude between timescales calculated from the two different tidal models of Goldreich & Sari (2009) and Jacobson & Scheeres (2011b). As expected, satellites with larger semi-major axes such as the outer satellites in 2001 SN263 and 1994 CC will have mutual orbits that take longer to circularize, and closer-in systems will have shorter damping timescales. The total possible lifetimes of each system, which includes collisional and dynamical lifetimes, are also listed in Table 2. For 1994 CC’s outer satellite, its orbit has a damping timescale that is clearly greater than its total possible lifetime. If this satellite formed from a post-fission dynamics scenario (Jacobson & Scheeres 2011) with a high post-fission eccentricity (~ 0.8), the system cannot evolve to the currently observed eccentricity of 0.19 by tides within its lifetime; this remains true even if there are Q differences between the primary and secondary (i.e. let $Q_p = 100$ and $Q_s = 10$) or if the satellite’s size is underestimated (its radius can be as large as 55 meters; Brozovic et al. 2011). If 1994 CC’s outer satellite is to be explained by post-fission dynamics and tides, then either fissioning can deliver a far-flung satellite with

lower eccentricities or the equations that idealize tidal interactions are not sufficient. For 1999 KW4, 2002 CE26, Didymos, 1991 VH, and 2001 SN263 #1, their ranges of damping timescales are less than their total possible lifetimes and this suggests that they should be close to circular, which is corroborated by the fact that their observed e are all less than 0.1. For most NEAs, we cannot draw firm conclusions since these calculations are very dependent on crucial parameters such as k and Q , which are poorly constrained for small asteroids; their damping timescales can be either greater or less than their total lifetimes.

To summarize, in this subsection we have considered the effect of tides in modifying eccentricity. Current models show that tides will damp eccentricity, but increasing eccentricity is possible if the primary and secondary have different density and/or Q values. The post-fission dynamics model of Jacobson & Scheeres (2011) tends to produce high- e in distant satellites, and we find that for all satellites except the outer satellite of 1994 CC, it is possible that tides can damp their post-fission eccentricities to observed eccentricities within a collisional lifetime.

2.2. Satellite's Spin Evolution

We consider a satellite's spin evolution due to tidal torques (on the tide-generated bulge as well as on the permanent deformation) and the radiative YORP effect. Spin evolution is important in our investigation on the origin of the observed spin states of NEA satellites as well as its consequences for spin-orbit synchronization-dependent processes such as BYORP.

In the absence of other perturbations, spin-orbit synchronization of the satellite is the fastest tidal process (Goldreich & Sari 2009) according to

$$\frac{d\omega_s}{dt} = 5\pi \text{sgn}(n - \omega_s) \frac{k_s}{Q_s} G \rho_p \left(\frac{\rho_p}{\rho_s} \right) \left(\frac{R_p}{a} \right)^6 \quad (2)$$

where ω is the spin rate, n is the mean motion, k is the Love number, Q is the tidal dissipation factor, G is the gravitational constant, ρ is the density, R is the radius, and a is the semi-major axis. Subscripts p and s denote the primary and satellite, respectively. All observed asynchronous satellites in our sample are fast rotators that spin faster than their orbital motions and so $d\omega_s/dt$ will be negative. We calculate the synchronization timescales τ_{sync} to despin from a breakup period (~ 2.33 hours) to its orbital period according to Equation 2, and present them in Table 3. These despinning timescales are shorter than the total lifetimes for most satellites and are shorter than the eccentricity damping timescales for all satellites (Table 2). These synchronization timescales will likely be affected by YORP, which may help speed up synchronization or slow it down.

Accordingly, we investigate the effect of YORP during a satellite's spin evolution. For both cases of an initially asynchronous or synchronous satellite, we ask, how does a satellite's rotation evolve when the semi-major axis changes? We do not assume that the orbit migration is dominated by any particular mechanism. Perturbations such as tides or BYORP can increase a satellite's semi-major axis, and BYORP can also decrease the semi-major axis.

2.2.1. Initially Asynchronous Satellite

First, we examine an initially asynchronous satellite, perhaps newly formed. All satellites will go through this stage. Its spin evolution will be affected by YORP as well as the torque due to the satellite's tidal bulge. The restoring torque due to the satellite's permanent deformation is not applicable in this case because this torque averages out unless the satellite is in a spin-orbit resonance (Murray & Dermott 1999).

We apply the torque equations due to tides raised on the satellite by the primary and YORP using the formalism given in Murray & Dermott (1999) and Steinberg & Sari (2011) for the magnitudes of the torques N :

$$N_{\text{tide}} = \frac{3}{2} \frac{k_s}{Q_s} \frac{GM_p^2 R_s^5}{a^6} \quad (3)$$

$$N_{\text{YORP}} = \frac{R_s^3 |f_Y| L_\odot}{6cd_\odot^2 \sqrt{1 - e_\odot^2}} \quad (4)$$

where G , c , and L_\odot are the gravitational constant, the speed of light, and the solar luminosity, respectively. The heliocentric parameters include semi-major axis d_\odot and eccentricity e_\odot . Tidal parameters include the Love number k_s and dissipation factor Q_s , where the subscript s denotes that these quantities are for the satellite. M_p is the primary's mass, a is the semi-major axis, and R_s is the satellite's radius. Following Goldreich & Sari (2009), we include a YORP reduction factor f_Y that can be positive or negative, and accounts for a reduction from its maximum possible value. This factor is necessary since the incoming radiation is not completely absorbed and reemitted tangentially along the satellite's equator.

The tidal torque will try to establish synchronization between the secondary's spin and its orbital period, and the YORP torque will perturb the secondary's spin in either direction. Their relative contributions are dependent on the semi-major axis. If the torques act in the same direction, the satellite's spin will synchronize with its orbital period. If the torques are competing, spin synchronization is not guaranteed. The critical semi-major axis $a_{c,\text{tide}}$ at which the magnitudes of these torques are equal is

$$a_{c,\text{tide}} = (3R_s M_p d_\odot)^{1/3} \left(\frac{k_s G c \sqrt{1 - e_\odot^2}}{Q_s |f_Y| L_\odot} \right)^{1/6} \quad (5)$$

where the constants and variables are the same as defined for Equations 3 and 4.

Satellites with orbital distances less than this critical semi-major axis $a_{c,\text{tide}}$ will become synchronous, whether or not YORP and tides act in the same direction. For orbital distances greater than the critical semi-major axis, satellites will likely remain asynchronous if tides and YORP act in opposite directions. We calculate $a_{c,\text{tide}}$ for all systems in our sample (Table 1), using $Q_s = 10 - 100$ and $f_Y \sim 5 \times 10^{-4}$ as suggested by observations of (54509) YORP (formerly 2000 PH5) (Lowry et al. 2007; Taylor et al. 2007). A list of $a_{c,\text{tide}}$ is given in Table 3. Uncertainties in the tidal Love number k_s and dissipation value Q_s produce a range of critical semi-major axes

Table 2
Tidal Timescales for Eccentricity Damping

System	a/R_p	e	τ_{lifetime} (yr)	τ_{damp} (yr):	
				$(k \propto R)^a$	$(k \propto R^{-1})^b$
2000 DP107	6.6	0.01	3.36×10^8	$1 \times 10^8 - 1 \times 10^9$	$4 \times 10^5 - 4 \times 10^6$
1999 KW4	3.9	0.008	4.32×10^8	$3 \times 10^6 - 3 \times 10^7 \ddagger$	$3 \times 10^4 - 3 \times 10^5$
2002 CE26	2.8	0.025	7.03×10^8	$1 \times 10^7 - 1 \times 10^8$	$4 \times 10^4 - 4 \times 10^5$
*2004 DC	4.4	0.30	2.19×10^8	$2 \times 10^8 - 2 \times 10^9$	$3 \times 10^4 - 3 \times 10^5$
*2003 YT1	7.1	0.18	3.94×10^8	$1 \times 10^9 - 1 \times 10^{10}$	$1 \times 10^6 - 1 \times 10^7$
Didymos	3.0	0.04	3.36×10^8	$5 \times 10^6 - 5 \times 10^7$	$4 \times 10^3 - 4 \times 10^4$
*1991 VH	5.4	0.06	4.12×10^8	$2 \times 10^7 - 2 \times 10^8$	$2 \times 10^5 - 2 \times 10^6$
2001 SN263 #1	2.9	0.016	6.06×10^8	$3 \times 10^6 - 3 \times 10^7 \ddagger$	$4 \times 10^4 - 4 \times 10^5$
*2001 SN263 #2	13	0.015	6.06×10^8	$4 \times 10^8 - 4 \times 10^9$	$4 \times 10^7 - 4 \times 10^8$
1994 CC #1	5.6	0.002	2.96×10^8	$5 \times 10^8 - 5 \times 10^9 \ddagger$	$1 \times 10^6 - 1 \times 10^7$
*1994 CC #2	20	0.19	2.96×10^8	$5 \times 10^{12} - 5 \times 10^{13} \ddagger$	$2 \times 10^9 - 2 \times 10^{10}$

For each system's satellite, we list the adopted values for the observed semi-major axis a/R_p and eccentricity e , its total possible lifetime τ_{lifetime} (collisional lifetime plus dynamical lifetime) (Bottke et al. 2005), and the eccentricity damping timescale τ_{damp} due to tides for synchronous satellites. We include two tidal models with a different size dependence of the Love number k . For each model, there is a range of values due to adopted values for the tidal dissipation factor $Q \sim 10-10^2$.

* Known asynchronous satellites

‡ Systems in which we assumed that all components had density equivalent to that of primary

^aGoldreich & Sari (2009)

^bJacobson & Scheeres (2011b)

Table 3
Tidal Timescales and Distances for Spin Synchronization

System	a/R_p	e	τ_{sync} (yr):		$a_{c,\text{tide}}/R_p$:		R_H (km)	$a_{c,\text{perm}}$ (km)
			$(k \propto R)^a$	$(k \propto R^{-1})^b$	$(k \propto R)^a$	$(k \propto R^{-1})^b$		
2000 DP107	6.55	0.01	$7 \times 10^6 - 7 \times 10^7$	$6 \times 10^4 - 6 \times 10^5$	2.88 - 4.23	6.33 - 9.28	86	1091
1999 KW4	3.86	0.008	$2 \times 10^5 - 2 \times 10^6$	$4 \times 10^3 - 4 \times 10^4$	2.80 - 4.12	5.36 - 7.86	70	1703
2002 CE26	2.78	0.025	$6 \times 10^4 - 6 \times 10^5$	$6 \times 10^2 - 6 \times 10^3$	2.80 - 4.11	6.14 - 9.01	514	4584
*2004 DC	4.41	0.30	$3 \times 10^6 - 3 \times 10^7$	$1 \times 10^3 - 1 \times 10^4$	1.41 - 2.06	5.24 - 7.65	44	189
*2003 YT1	7.15	0.18	$1 \times 10^7 - 1 \times 10^8$	$4 \times 10^4 - 4 \times 10^5$	2.67 - 3.93	6.62 - 9.71	113	1488
Didymos	2.95	0.04	$8 \times 10^4 - 8 \times 10^5$	$2 \times 10^2 - 2 \times 10^3$	2.30 - 3.38	6.35 - 9.33	109	891
*1991 VH	5.43	0.06	$1 \times 10^6 - 1 \times 10^7$	$3 \times 10^4 - 3 \times 10^5$	3.40 - 5.00	6.38 - 9.37	105	1987
2001 SN263 #1	2.92	0.016	$1 \times 10^5 - 1 \times 10^6$	$2 \times 10^3 - 2 \times 10^4$	3.40 - 4.99	6.46 - 9.48	343	5415
*2001 SN263 #2	12.8	0.015	$7 \times 10^7 - 7 \times 10^8$	$8 \times 10^6 - 8 \times 10^7$	5.16 - 7.58	7.43 - 10.9	343	5532
1994 CC #1	5.58	0.002	$2 \times 10^7 - 2 \times 10^8$	$3 \times 10^4 - 3 \times 10^5$	2.03 - 3.00	6.16 - 9.06	86	911
*1994 CC #2	19.8	0.19	$3 \times 10^{10} - 3 \times 10^{11}$	$2 \times 10^7 - 2 \times 10^8$	1.71 - 2.52	5.81 - 8.55	86	553

For each system's satellite, we list the adopted values for the observed semi-major axis a/R_p and eccentricity e , the tidal spin synchronization timescale τ_{sync} starting from the breakup rate in the absence of other effects such as YORP, the critical semi-major axis $a_{c,\text{tide}}/R_p$ within which an initially asynchronous satellite can achieve synchronization against the effects of YORP torques that compete with tidal torques, Hill radii R_H , and an upper limit to the critical semi-major axis $a_{c,\text{perm}}$ at which an initially synchronous satellite would break spin lock due to the effects of YORP. The critical semi-major axes are calculated using $f_Y \sim 5 \times 10^{-4}$. When applicable, we include 2 tidal models with a different size dependence of the Love number k . For each model, there is a range of values due to adopted values for the tidal dissipation factor $Q \sim 10-10^2$.

* Known asynchronous satellites

^aGoldreich & Sari (2009)

^bJacobson & Scheeres (2011b)

per NEA binary in our sample, and different values for f_Y would result in an even broader range.

We now discuss the agreement between our calculations of $a_{c,\text{tide}}$ and the observed spin states (given in Table 3) of NEA satellites in our sample. Two satellites, 2002 CE26’s secondary and 2001 SN263’s inner satellite, have current semi-major axes less than the range of possible $a_{c,\text{tide}}$ values calculated in this table, and they are both observed to be synchronous. Two satellites, the outer satellites of 2001 SN263 and 1994 CC, have current semi-major axes larger than their range of possible $a_{c,\text{tide}}$ values, and they are both observed to be asynchronous; this suggests that tides and YORP act in opposing directions for these two satellites. All other satellites whose current semi-major axes may or may not be larger than their $a_{c,\text{tide}}$ include synchronous and asynchronous rotators. The dominance of YORP for satellites such as 2001 SN263 #2 explains how it could have a tidally-circularized orbit yet be asynchronous.

Further observations of asynchronous satellites can help constrain which tidal model (Goldreich & Sari 2009; Jacobson & Scheeres 2011b) best captures the behavior of small bodies, assuming that tides and YORP are the dominant processes affecting satellite spin states. For this test we focus on asynchronous satellites because in that case the balance of tidal and YORP torques requires their observed semi-major axes to be larger than their computed $a_{c,\text{tide}}$ values. Comparison of the observed a to the predicted $a_{c,\text{tide}}$ for a number of asynchronous satellites of different sizes may reveal which tidal model is more appropriate. We encourage observations of asynchronous satellites to enable this test. Unfortunately the same test cannot be applied to the more numerous synchronous satellites because their spin can be explained by tides and YORP torques acting in the same direction with the observed $a < a_{c,\text{tide}}$ or $a > a_{c,\text{tide}}$, or by tides and YORP acting in opposite directions with $a < a_{c,\text{tide}}$.

2.2.2. Initially Synchronous Satellite

We now consider the case of an initially synchronous satellite. Its spin evolution will be affected by YORP, the satellite’s tidal bulge, and additionally, a restoring torque due to the satellite’s permanent deformation. The permanent quadrupole moment of the satellite plays a role for spin states in spin-orbit resonance and is thus applicable when considering the spin evolution of a synchronous satellite. The expression for the magnitude of the torque due to permanent deformation is given by Murray & Dermott (1999) as

$$N_{\text{perm}} = \frac{3}{2}(B - A) \frac{GM_p}{a^3} \sin(2\psi) \quad (6)$$

where B and A are the satellite’s equatorial principal moments of inertia, G is the gravitational constant, M_p is the mass of the primary, a is the semi-major axis, and ψ is the amplitude of the libration.

We compare the tidal torque N_{tide} to the permanent deformation torque N_{perm} for the case of 1999 KW4, which is currently the only NEA binary with published shape information of the secondary. Using 1999 KW4’s $(B - A)$ value for its secondary, $\psi \sim \pi/4$ (maximum amplitude), values for Q from 10 to 100, and both tidal models (Goldreich & Sari 2009; Jacobson & Scheeres 2011b),

we find that N_{perm} dominates over N_{tide} by at least six orders of magnitude. Therefore, for the case of an initially synchronous satellite that we examine here, we will consider only the permanent deformation torque (and not the torque on the tidal bulge) as well as the YORP torque. The permanent deformation torque will seek to maintain spin-orbit synchronization, and the YORP torque will attempt to spin the satellite in either direction away from synchronization. Balance of the permanent deformation and YORP torques yields a critical semi-major axis $a_{c,\text{perm}}$ given as

$$a_{c,\text{perm}} = \frac{1}{R_s} \left(\frac{9(B - A)GM_p \sin(2\psi)cd_{\odot}^2 \sqrt{1 - e_{\odot}^2}}{|f_Y|L_{\odot}} \right)^{1/3} \quad (7)$$

where the constants and variables are the same as defined for Equations 4 and 6.

In the absence of significant eccentricities, this critical semi-major axis $a_{c,\text{perm}}$ separates regions where synchronization can be maintained and where synchronization can be broken. We seek an upper limit for $a_{c,\text{perm}}$ to determine if synchronization can be maintained to distances as large as the Hill radius, which is a requirement for synchronization-dependent processes such as BYORP to create asteroid pairs. In Table 3, we present calculations of an upper limit $a_{c,\text{perm}}$ for all satellites in our sample. We adopt a maximum libration amplitude $\psi \sim \pi/4$ and calculate $(B - A)$ for each satellite by scaling from the $(B - A)$ of one of the most elongated NEAs known, Geographos (Ostro et al. 1995):

$$(B - A)_x = \frac{(B - A)_{\text{Geo}}}{M_{\text{Geo}}R_{\text{Geo}}^2} M_x R_x^2 \quad (8)$$

where subscripts x and Geo represent the considered satellite and Geographos, respectively. The mass is M and the equivalent radius (if it were spherical) is R . The equivalent radius of Geographos is ~ 1.28 km (Hudson & Ostro 1999), and if we assume a typical rubble pile density of 2 g cm^{-3} , its mass is $\sim 1.8 \times 10^{13}$ kg. Using a triaxial ellipsoid assumption to calculate its moments of inertia, we find $(B - A)_{\text{Geo}}/(M_{\text{Geo}}R_{\text{Geo}}^2)$ to be ~ 0.56 . Similarly as we did earlier for calculations of $a_{c,\text{tide}}$, we adopt $f_Y \sim 5 \times 10^{-4}$. These values are used in the calculation of an upper limit $a_{c,\text{perm}}$ shown in Table 3.

Table 3 shows that for all NEA systems, $a_{c,\text{perm}}$ is much larger than the Hill radius. This suggests that once a satellite has synchronized its spin to its orbital period, it can remain so out to far distances even in the presence of YORP. Therefore, all observed asynchronous satellites (2004 DC, 2003 YT1, 1991 VH, and the outer satellites of triples 2001 SN263 and 1994 CC) have probably never been synchronous unless they experienced a planetary encounter that disrupted their synchronous spins.

An alternative proposal was recently put forth by Jacobson & Scheeres (2011a), who suggest that longitude librations of the satellite will occur about a direction that is not aligned with the line connecting the central body and the satellite. They hypothesize that this angular offset becomes increasingly significant as the orbit expands (due to tides and BYORP), and eventually results in breaking a satellite’s spin lock. If this model is

correct, then synchronization cannot be maintained to far distances. However this model seems to produce substantial angular offsets only for satellites with very small moment of inertia differences ($(B - A)/C$), and therefore does not appear to be effective for the overwhelming majority of satellites.

To summarize, we find that a newly post-fissioned, asynchronous satellite can become synchronous within its lifetime and this can explain all observed synchronous and circular binaries and inner satellites of triples. Asynchronous outer satellites in both triples are unable to synchronize by tidal torques because of the larger influence of YORP, and this may also be the explanation for asynchronous binaries 2004 DC, 2003 YT1, and 1991 VH. The dominance of YORP over tides at large distances may explain why the outer satellite in 2001 SN263 remains asynchronous despite having an orbit that appears to have tidally circularized.

2.3. *Semi-major Axis Evolution*

The post-fission dynamics model of Jacobson & Scheeres (2011) shows how satellites can be deposited at large separations up to ~ 16 primary radii (Section 1.3) and can explain the outer satellite in 2001 SN263 (at ~ 13 primary radii) and perhaps also the outer satellite in 1994 CC (at ~ 20 primary radii). Here we investigate if another mechanism, namely tidal evolution, can bring satellites from closer-in to wide orbits.

To explore this possibility, we study three cases of wide orbits: 2001 SN263 #2, 1994 CC #2, and we also consider a hypothetical wide binary modeled after 1998 ST27, which has a primary radius of 0.42 km and a lower limit on its observed semi-major axis of 5 km. For these three systems, we calculate the tidal timescales for the semi-major axis to increase from one primary radius to its observed value. For both tidal models (Goldreich & Sari 2009; Jacobson & Scheeres 2011b) and using $Q = 10\text{--}100$, we find that the tidal timescales for such increases in semi-major axis are $\sim 10^9\text{--}10^{10}$ years for 2001 SN263 #2, $\sim 10^{10}\text{--}10^{13}$ years for 1994 CC #2, and $\sim 10^9\text{--}10^{11}$ for the hypothetical wide binary modeled after 1998 ST27. The total possible lifetimes of these satellites (see Table 2; for the hypothetical binary, its lifetime is $\sim 3.4 \times 10^8$ years) are shorter than their tidal expansion timescales. This suggests that tides cannot account for the wide orbits of these satellites, if the tidal model is correct. Other influencing factors such as “tidal saltation,” the idea of mass lofting from the primary and briefly entering into orbit to transfer orbital angular momentum to the satellite before falling back down to the primary’s surface, may speed up tidal expansion (Harris et al. 2009).

Next, we investigate if tides can explain the wide orbits by using different assumptions of interior properties. Assuming tidal dissipation Q values of $10\text{--}100$, we calculate their material properties in order for their semi-major axes to increase from one primary radius to the currently observed semi-major axis within their NEA-specific lifetimes. We find that in order for tides to be responsible for the increase in semi-major axis within the considered system’s lifetime, we will need to invoke the following values for k_p : $\sim 0.00003\text{--}0.00030$ for 2001 SN263 #2, $\sim 0.0054\text{--}0.0545$ for 1994 CC #2, and $\sim 0.00028\text{--}0.00285$

for the hypothetical binary modeled after 1998 ST27. The required k value for 1994 CC #2 is prohibitive and is almost as large as or larger than the Moon’s k of 0.025 (Williams et al. 2008).

In summary, tidal evolution cannot explain the semi-major axes of widely-separated systems without invoking unusual material properties, lower Q values than assumed, a different tidal model, or a combination of these factors. Our analysis here supports the idea that post-fission dynamics may be largely responsible for some of the wide orbits observed in NEA systems.

3. BYORP EVOLUTION

The BYORP effect occurs for a synchronously rotating satellite with an asymmetrical shape. A synchronous satellite has permanent leading and trailing hemispheres, and an asymmetrical shape will result in re-radiation of absorbed sunlight that is uneven between the two hemispheres. This disparity results in a net acceleration (or deceleration) of the satellite’s orbit and can therefore cause orbital evolution. This effect has not been observationally verified, and in this section we evaluate BYORP’s relevance in explaining the observed spin-orbital characteristics of NEA systems by introducing current theoretical models predicting BYORP’s effects and timescales.

For all observed asynchronous satellites, we rule out BYORP as a major player in their recent evolution because this effect depends on spin-orbit synchronization; without synchronous spin, the effect cancels out. This is applicable to nearly half of the satellites in our sample that are asynchronous (Table 1): 2004 DC, 2003 YT1, 1991 VH, 2001 SN263 #2, and 1994 CC #2. We now examine scenarios in which BYORP may have had an important role in the past evolutionary histories of these systems, assuming their satellites used to be synchronous.

First, we consider the case where a synchronous satellite evolved via BYORP and broke spin-lock through a planetary encounter. Such a scenario would imply that its past BYORP-affected orbital properties would be erased in part by the scattering encounter; therefore, any observed properties cannot be wholly attributed to BYORP, but would also be attributed to the flyby.

Second, we consider the case where BYORP expands a synchronous satellite’s orbit and increases the eccentricity enough to break spin-lock and result in chaotic asynchronous rotation (Ćuk & Nesvorný 2010). This could perhaps explain the observed eccentric and asynchronous satellites, but we find this unlikely for two reasons. First, synchronous re-capture is thought to occur rapidly (Ćuk & Nesvorný 2010, on the order of $\sim 10^3$ years) and would prevent a substantial population of asynchronous binaries from forming. Second, this process would not explain how all observed asynchronous satellites acquired spin periods much less than their respective orbital periods.

In essence, although we cannot rule out that BYORP played a role in the evolution of asynchronous satellites, we find that tides (for spin synchronization) or planetary encounters are required to explain the data, whereas BYORP is not. Therefore, we find that BYORP alone cannot explain the properties of asynchronous satellites, which includes all satellites with large semi-major axes.

We apply the same reasoning to widely-separated systems such as 1998 ST27 and the outer satellites of the triples. Because neither tides alone nor BYORP alone can readily explain the origin of large semi-major axes, we conclude that these properties may be primarily a result of post-fission dynamics rather than evolutionary processes.

For all remaining synchronous satellites, BYORP may be responsible for their observed spin-orbital characteristics. However, BYORP is neither necessary nor sufficient to explain these properties: another evolutionary process (tides) is required to first synchronize the satellite’s spin before BYORP can operate. BYORP’s relevance for NEA systems is also complicated by the short BYORP timescales. An important unresolved issue with our understanding of BYORP has to do with conflicting models on the sign of de/dt with respect to da/dt . These issues are discussed in the following paragraphs.

Current theories predict different behaviors of semi-major axis and eccentricity evolution due to BYORP (Goldreich & Sari 2009; Čuk & Nesvorný 2010; McMahon & Scheeres 2010a,c; Steinberg & Sari 2011). McMahon & Scheeres (2010a) describe how the overall orbital evolution over long timescales due to BYORP causes the semi-major axis and eccentricity to evolve in *opposite directions*, even with the inclusion of libration effects. Čuk & Nesvorný (2010) also include the effects of a secondary’s librations due to its elongated shape and predict that librations dominate over direct perturbations by BYORP. They describe how the semi-major axis and eccentricity evolve in the *same direction*. They suggest that the most likely outcome of an initially expanding orbit (with $\dot{e} > 0$ in their model) is chaotic rotation of the secondary followed by synchronous spin re-establishment and inward migration, which would prevent evolution to large semi-major axes. Steinberg & Sari (2011) also find that the preferred end state for BYORP is shrinkage of the semi-major axis. On the other hand, McMahon & Scheeres (2010b) suggest that librational motion for binaries like 1999 KW4 ($\sim 5^\circ$ amplitude librations; Ostro et al. 2006) will remain small for expanding orbits (with $\dot{e} < 0$ in their model), preventing chaotic rotation of the secondary, and leading to large semi-major axes. Future measurements of spin states of satellites can help constrain which model best captures the correct behavior.

The timescales for BYORP evolution are thought to be fast. Čuk & Burns (2005) find that for most asteroid shapes, the BYORP torque is significant and can modify the satellite’s orbital semi-major axis and eccentricity on timescales of $\sim 10^5$ years. Similar expansion timescales have been found by McMahon & Scheeres (2010a), who assert that orbits can typically expand to their Hill sphere due to BYORP on the order of $10^4 - 10^6$ years. Currently, 1999 KW4 is the only well-characterized NEA binary with published shapes of both primary and secondary, and McMahon & Scheeres (2010a) predict an orbit expansion rate of 7 cm yr^{-1} (a prediction corroborated by Steinberg & Sari (2011)) and an orbit-doubling time of $\sim 22,000$ years. Under the influence of BYORP, primary oblateness, and solar perturbations, they predict that 1999 KW4 will reach its Hill radius in $\sim 54,000$ years. Incorporation of librational effects into the model

by McMahon & Scheeres (2010a) causes a longer BYORP evolution, but the mutual orbit will still expand to its Hill radius for small librational motion to at least 12° (McMahon & Scheeres 2010b).

There are potential puzzles with the hypothesized short BYORP timescales and assertions that BYORP-induced orbit expansion can reach the Hill radius. First, binary formation would need to be rapid enough to produce the observed fraction of NEAs with satellites. Since NEAs have dynamical lifetimes on the order of a few million years (Bottke et al. 2002), much larger than the BYORP disruption timescale of ~ 0.1 million years, the binary production rate would need to match the rate of binaries disrupted by BYORP for a steady-state binary NEA population. Part of this issue (at least for nominally half of all systems in which BYORP causes inward migration) may be mitigated if a stable equilibrium exists between BYORP and tides (e.g. Jacobson & Scheeres 2011b). If BYORP acts to contract the orbit and tides cause expansion of the orbit, there is a critical semi-major axis at which their effects may balance and result in a stable equilibrium. Second, according to McMahon & Scheeres (2010a), BYORP can expand the orbits (nominally half) of satellites to their Hill radii. This means we should observe some systems that are at significant fractions of their Hill radii; for instance, the Hill radii of these systems are typically a few hundred primary radii. However, we do not observe any systems wider than 20 primary radii. Moreover, such BYORP-induced expansion to the Hill sphere will cause the expanding binary to become more susceptible to planetary encounters by shortening the encounter timescale and strengthening the perturbative effects of encounters. Using equations and timescales in Fang & Margot (2011), we calculate that if 1999 KW4 reaches a separation halfway to its Hill radius, Earth encounters at a typical encounter velocity of 12 km s^{-1} are expected to disrupt the binary at encounter distances of ~ 28 Earth radii, which can occur every $\sim 260,000$ years. With a separation of 90% of its Hill radius, disruptive encounters can occur every $\sim 100,000$ years. As a result, we suggest that planetary encounters may also create asteroid pairs in the near-Earth population.

We also mention that the predictions for 1999 KW4’s expansion to its Hill radius given by McMahon & Scheeres (2010a) are not ruled out by our calculations of upper limit critical semi-major axes $a_{c,\text{perm}}$ at which a synchronous satellite will have its spin lock broken. We calculated these critical semi-major axes (Table 3) using Equation 7, which compares the torque due to a satellite’s permanent deformation (which maintains synchronization in the absence of significant eccentricities) and the torque due to YORP (which can spin an asteroid away from synchronization). Table 3 shows that for all NEA satellites, the critical semi-major axis $a_{c,\text{perm}}$ is much larger than the Hill radius, meaning that synchronization can be maintained in the absence of other perturbations. Thus, if the predictions by McMahon & Scheeres (2010a) are correct (i.e. eccentricities remain small when the orbit expands), the formation of asteroid pairs by BYORP-induced orbit expansion (and possibly planetary encounters) is possible.

To summarize, we find that BYORP is not currently

acting for nearly half of the satellites in our sample of NEA binaries and triples because they are asynchronously rotating. We also find difficulties associated with the hypothesis that BYORP operated in the past evolutionary histories of these currently asynchronous satellites, although we cannot rule out that their orbital properties may have been shaped in part by BYORP. For the remaining synchronous satellites, BYORP may be acting but is not required to explain observed orbital properties.

4. EVOLUTION BY CLOSE PLANETARY ENCOUNTERS

In this section, we examine if close planetary encounters can explain the observed spin-orbital properties of well-characterized NEA systems.

The majority of satellites in our sample of NEA systems are synchronously rotating and on near-circular orbits. This includes 2000 DP107, 1999 KW4, 2002 CE26, Didymos, and the inner satellites of 2001 SN263 and 1994 CC. We find that close planetary encounters are unlikely to explain these properties. We expect that planetary encounters are strong enough to cause changes to an asteroid’s spin state (e.g. Scheeres et al. 2000, 2004) and orbital eccentricity (e.g. Fang & Margot 2011), such that we would not expect a majority of synchronous and circular binaries if planetary flybys were a dominant process. Similarly, planetary flybys are also not likely to explain the spin-orbital state of 2001 SN263’s outer satellite, which although asynchronous, has a circular orbit.

For asynchronous binaries 2003 YT1, 2004 DC, and 1991 VH, their eccentricities are 0.18, 0.3, and 0.06, respectively. The outer satellite of 1994 CC is also asynchronous with an orbital eccentricity of 0.19. 2003 YT1, 2004 DC, and 1991 VH have semi-major axes that indicate their expected eccentricities following post-fission dynamics were higher or comparable to their current eccentricities (Figure 2). If they formed at their current semi-major axes, either tides did not have sufficient time to damp the eccentricities to circular orbits (Table 2), or a planetary encounter may have erased some of the tidal damping effects by increasing the eccentricities. If they formed closer-in (with correspondingly lower eccentricities following post-fission dynamics), a planetary encounter may have increased both their semi-major axis and tidally-damped eccentricity to observed values. 1994 CC’s outer satellite has tidal damping timescales much longer than its total possible lifetime, and so its current eccentricity is too low to be explained by post-fission dynamics and tides. In this case, it is possible that planetary encounters may have lowered its eccentricity from a high predicted value following post-fission dynamics to its observed value.

To investigate these scenarios, we employ results from a companion paper on the effect of planetary encounters with binary asteroids (Fang & Margot 2011). We find that for a planetary flyby to increase each of the asynchronous binaries’ eccentricities from a tidally-damped value of 0 to its observed value would take ~ 4.94 Myr for 2003 YT1, ~ 6.54 Myr for 2004 DC, and ~ 0.56 Myr for 1991 VH. These encounter timescales represent the average time for an eccentricity increase when the binary is in near-Earth space, assuming the NEA follows a trajectory from main belt source regions to its current orbit in near-Earth space. These timescales can occur within

the near-Earth dynamical lifetime on the order of a few million years. Inclusion of additional planets and repeat passes will make it more likely that planetary encounters can affect orbital properties (see Fang & Margot (2011) for details). For the case of 1994 CC with a starting eccentricity of 0.8, the largest decreases in eccentricity happen for shorter encounter distances. However, at shorter encounter distances, unstable encounters with collisions and ejections dominate. For instance, at an encounter distance of 2 Earth radii, the average post-encounter eccentricity is ~ 0.58 (not low enough to match the observed eccentricity of 0.19) and the percentage of stable encounters is less than 1%. Smaller encounter distances are even more problematic. Scenarios with repeat passes, where the eccentricity has a net decrease to its observed value, are also very unlikely. Therefore, our results suggest that planetary encounters cannot decrease the orbital eccentricity of 1994 CC’s outer satellite from high values to moderate values.

Next, we investigate if the widest orbits observed in NEA systems originate from post-fission dynamics (Section 1.3 and Figure 2) or possibly another mechanism, namely planetary encounters. We examine a hypothetical binary modeled after 1998 ST27 with a large separation of ~ 16 primary radii and an eccentricity of 0.3. Our simulations used encounter distances of $2\text{--}12 R_{\oplus}$ and encounter velocities of $8\text{--}24 \text{ km s}^{-1}$ for an Earth-mass perturber. We find that encounters cannot create wide systems, except very rarely. Here are a few illustrative cases we examine:

1. We perform simulations starting with a circular binary with a separation of 4 primary radii, which is typical for NEA binaries. For a typical encounter velocity of 12 km s^{-1} , encounters at a distance of $8 R_{\oplus}$ showed that $\sim 7\%$ of stable encounters at least doubled in semi-major axis and none of the stable binaries quadrupled in semi-major axis. Encounters resulting in stable binaries that at least doubled in semi-major axis had post-flyby eccentricities of $\gtrsim 0.45$, which is larger than any observed eccentricity but may damp within a dynamical lifetime.

2. We perform a “repeat encounter” scenario starting with an eccentric binary ($e = 0.5, 0.7$) with a separation of 8 primary radii. These initial conditions assume that an a priori encounter already doubled the semi-major axis from 4 to 8 primary radii and increased the eccentricity to high values. We find that it is possible to both decrease the eccentricity and further increase the semi-major axis to observed values. However, this only occurred in $\sim 5\%$ of stable encounters with a fine-tuned initial semi-major axis and eccentricity in order to match the observed values.

3. We investigate if this hypothetical wide binary used to be a triple system by performing simulations of a primary asteroid and 2 satellites initially located at 4 and 16 primary radii with circular orbits. The chance of ejecting the inner satellite with the outer satellite intact is possible, but only occurs in $\lesssim 3\%$ of all unstable encounters with encounter distances less than $\sim 8 R_{\oplus}$. When it does happen, the final eccentricity of the outer satellite is typically higher than any observed eccentricity.

Our work shows that planetary encounters are not necessary to explain the observed spin-orbital properties of binary NEAs, but in reality, close planetary encounters will occur and they will change the orbital characteris-

tics of NEA multiples (Fang & Margot 2011). To reconcile these two results, there are a few possibilities: (a) the observed synchronous and circular systems are more recent migrants to near-Earth space that have not yet undergone deep planetary encounters, and oppositely, the asynchronous and eccentric systems have been interacting with planets for longer periods of time, or (b) the observed systems have encountered terrestrial planets, but tidal evolution occurs on a faster timescale, and has managed to synchronize and circularize some systems. Possibility (b) may or may not be supported by calculations of tidal damping timescales (Table 2) depending on the tidal Love number model and NEA-specific encounter timescales.

In summary, we find that planetary encounters cannot explain observed synchronous satellites nor nearly circular orbits. For asynchronous satellites with non-circular orbits (2004 DC, 2003 YT1, and 1991 VH), we find that planetary encounters are a plausible explanation that can reproduce their observed eccentricities, although not necessary to explain the data (observed properties can be explained by tides alone). However, planetary encounters cannot decrease 1994 CC’s eccentricity from a high post-fission dynamics value to the observed value. We also find that the observed wide orbits were unlikely to be reached through planetary encounters.

5. EVOLUTION BY KOZAI RESONANCE

Now we examine orbital evolution by the Kozai resonance (Kozai 1962) by reviewing its effects and timescales as well as its applicability to observed NEA systems.

Kozai resonance (Kozai 1962) is a secular effect causing angular momentum exchange between an inner body’s orbital eccentricity and relative inclination with a massive, outer perturber. In this resonance, eccentricity e and inclination I are coupled, and the quantity $\sqrt{1 - e^2} \cos I$ is conserved in the idealistic case of an outer perturber with a circular orbit. For an initially circular binary, large Kozai oscillations can occur if the relative inclination between the inner and outer orbits is at least ~ 39.2 degrees, and this critical inclination depends on the ratio of their semi-major axes. Since this mechanism can result in high eccentricities, we consider Kozai resonance between an NEA binary and the Sun as the outer perturber (Perets & Naoz 2009). Triple systems are not considered here, as Fang et al. (2011) have shown that the presence of a second satellite damps any Kozai oscillations in the system and thus will not be a relevant mechanism in modifying the satellites’ eccentricities.

For binaries under the influence of the Kozai mechanism, we can estimate the Kozai period P_{Kozai} or typical oscillation timescale between limiting values of e and I as (Kiseleva et al. 1998)

$$P_{\text{Kozai}} = \frac{2P_{\odot}^2}{3\pi P_{\text{binary}}} (1 - e_{\odot}^2)^{3/2} \frac{M_p + M_s + M_{\odot}}{M_{\odot}} \quad (9)$$

where P_{\odot} is the heliocentric orbital period, P_{binary} is the binary’s mutual orbital period, and e_{\odot} is the heliocentric eccentricity. The binary’s primary mass is M_p , the secondary mass is M_s , and the outer perturber’s mass is the Sun’s mass (M_{\odot}) in the situation we examine here. In the absence of other effects, we calculate the Kozai peri-

ods for all well-characterized NEA binaries and present them in Table 4. Binaries with small heliocentric distances and/or large heliocentric eccentricities (such as 1999 KW4) have short oscillation periods. The very short timescales in Table 4 indicate that evolution by the Kozai mechanism is faster than any other evolutionary process examined in this study.

Determination of whether binaries are in the Kozai regime or not can be assessed for at least 2 near-circular binaries in our sample, 2000 DP107 and 1999 KW4, for which we have detailed information about the orientation of the mutual orbital plane. For these binaries, we calculate the current inclination between the binary’s mutual orbit and the Sun’s apparent orbit. We find that neither 1999 KW4 nor 2000 DP107 have inclinations that meet the critical Kozai angle. Other binaries in our sample do not currently have reliable orbital orientations. The difficulty of measuring precise orbital plane orientations without sufficient radar coverage makes the assessment of Kozai influences difficult to verify at the moment, and additional observations of NEA binaries are encouraged.

Fulfillment of the required Kozai inclination will be affected by processes that can change the relative inclination between the binary’s mutual orbit and its heliocentric orbit. For a satellite in an equatorial orbit with a semi-major axis of several primary radii, Čuk & Burns (2005) describe a possible equilibrium state where YORP and BYORP torques balance. They describe how this scenario can occur when the inclination between the primary’s equatorial plane and the heliocentric orbit is ~ 50 – 60 degrees. If the binary’s mutual orbit is in the same plane as the primary’s equator (as would be expected from the generally accepted rotational fission formation model), then the stable inclination of ~ 50 – 60 degrees would be the angle between the binary orbit and heliocentric orbit. Steinberg & Sari (2011) describe a different stable inclination that will be reached under the effects of BYORP, which will tend to orient a binary’s orbit into an inclination of either 0 or 90 degrees relative to its heliocentric orbit. However, we note that in the absence of Kozai-damping processes, a “stable” inclination of ~ 50 – 60 or 90 degrees would cause a binary to undergo Kozai cycles. Although the value of the stable inclination is unclear due to different predictions by Čuk & Burns (2005) and Steinberg & Sari (2011), we suggest that radiative torques may cause a binary that is initially not affected by Kozai effects to enter the Kozai regime when its relative inclination with the Sun’s apparent orbit is sufficiently high.

Next, we consider the effect of primary oblateness (described by a J_2 term) in modulating the Kozai effect for NEA binaries. The critical semi-major axis a_{c,J_2} for the transition between the influence regions of primary oblateness and solar dynamics such as the Kozai resonance is (Nicholson et al. 2008)

$$a_{c,J_2} = \left(2J_2 \frac{M_p}{M_{\odot}} R_p^2 a_{\odot}^3 \right)^{1/5} \quad (10)$$

where J_2 approximates the non-spherical shape of the primary by its level of oblateness, M_p is the mass of the primary, M_{\odot} is the mass of the Sun, R_p is the primary’s radius, and a_{\odot} is the heliocentric semi-major axis. We calculate a_{c,J_2} for all NEA binaries in our sample for J_2

Table 4
Kozai Oscillation Periods

Binary	a (km)	e	P_{Kozai} (yr)
2000 DP107	2.62	0.01	89.11
1999 KW4	2.55	0.008	10.78
2002 CE26	4.87	0.025	756.60
*2004 DC	0.75	0.30	269.78
*2003 YT1	3.93	0.18	58.40
Didymos	1.18	0.04	545.99
*1991 VH	3.26	0.06	81.34

For each binary, adopted values for the observed semi-major axis a and eccentricity e as well as the Kozai oscillation period P_{Kozai} are listed.

* Known asynchronous satellites

values ranging from 0.001 to 0.1, and we find that the range of possible a_{c,J_2} values is larger than the observed semi-major axis for all binaries. This implies that these binaries are dominated by primary oblateness, which will cause orbital precession that can completely suppress Kozai cycles.

Lastly, we note that this mechanism can alter an NEA binary’s spin state and eccentricity, but cannot change the semi-major axis of the binary’s mutual orbit in the averaged problem. Therefore, it cannot explain the observed wide orbits, which again suggests that these large separations are inherited from post-fission dynamics.

To summarize, Kozai resonance is not applicable for systems where its effects may be damped, and this includes all satellites in triple systems and binaries where primary oblateness may dominate. This includes all systems in our sample of well-characterized binaries and triples. The averaged Kozai effect also cannot modify the semi-major axis.

6. COMBINED ORIGIN AND EVOLUTION OF SPIN-ORBITAL PROPERTIES

Here we summarize the relevance of each evolutionary process examined in this study (tides, BYORP, planetary encounters, and Kozai effects) in the context of explaining the origin of observed spin-orbital properties of NEA systems in our sample (Table 1). Then we discuss evolutionary pathways between observed spin-orbital states and disrupted binaries (asteroid pairs and contact binaries).

Table 5 shows how each considered evolutionary process matches up against each other in explaining the spin-orbital origin of binaries and triples in our sample. Tidal evolution is a dominant process that can explain the satellite’s spin state and orbital eccentricity for nearly all systems assuming formation by rotational fission followed by post-fission dynamics. All other examined processes either depend on tidal evolution and/or are not required to explain the observed systems. For instance, BYORP requires a tidally-synchronized system to operate. Although BYORP is not required to explain the data, it may be acting in synchronous systems or may be pivotal in a stable equilibrium state where the effects of tides and BYORP cancel (i.e. Jacobson & Scheeres 2011b). Flybys, or planetary encounters, can potentially explain several asynchronous and non-circular systems, but not the majority of circular and synchronous systems. The Kozai

effect is not applicable for primary oblateness-dominated NEA systems in our sample. We also find that observed wide orbits, such as those of binary 1998 ST27 and the outer satellites of 2001 SN263 and 1994 CC, are most likely a direct byproduct of post-fission dynamics (Jacobson & Scheeres 2011) because none of the four evolutionary processes as currently modeled seem capable of delivering satellites to such large separations.

Now we discuss these evolutionary processes as an ensemble of pathways between spin-orbital states and disrupted states such as asteroid pairs and contact binaries. These pathways are shown in Figure 3 with the assumption that these systems are not affected by the Kozai effect. In the figure, the yellow box is the starting point for a rotationally fissioning asteroid. Green boxes represent potential outcomes. The evolutionary pathways are drawn in solid black (for post-fission dynamics), solid gray (for planetary encounters), and dotted black (for BYORP), with red lines representing differences between the two different BYORP models. Čuk & Nesvorný (2010) predict that BYORP-induced change in eccentricity has the same direction as the semi-major axis change (i.e. when the semi-major axis increases, the eccentricity increases). McMahon & Scheeres (2010a,c) predict that the eccentricity moves in the direction opposite to the semi-major axis change (i.e. when the semi-major axis increases, the eccentricity decreases).

As adopted in Figure 3, the term *asynchronous* can refer to two types of states where the satellite’s spin is non-resonant with its orbital period: “quasiperiodic” rotation, which is stable, and “chaotic” rotation, which is unstable. When these spin state trajectories are depicted on surface of section plots, “quasiperiodic” trajectories are smooth curves and “chaotic” trajectories are random points filling in an area on the plot. The stable or unstable nature of an asynchronous rotation can be readily discerned on such surface of section plots, as discussed in Murray & Dermott (1999) and shown for Saturn’s satellite Hyperion in Wisdom et al. (1984). A satellite’s principal moments of inertia $(B - A)/C$ determine the strength of spin-orbit resonances. The higher the eccentricity, the lower the necessary $(B - A)/C$ at which chaotic rotation can occur. An increase in eccentricity (due to perturbations such as BYORP) can lead to overlap between spin-orbit resonances. Simultaneous libration in more than one spin-orbit resonance is not possible, and this leads to chaotic behavior. A satellite can depart an unstable, “chaotic” state by reaching a stable “quasiperiodic” state and temporarily re-establish synchronization. In some models, this allows BYORP to regain control of the system and evolve it away from the chaotic states, as shown in simulations for 1999 KW4-like binaries by Čuk & Nesvorný (2010).

In Figure 3, we discuss spin-orbital pathways that are common to both BYORP models (lines not shown in red). Post-fission dynamics (<1000 years) combined with tidal dissipation (and possibly BYORP) can produce many observed examples of NEA systems, including both synchronous and asynchronous rotators, both circular and eccentric orbits, contact binaries, and asteroid pairs. Evolution between spin-orbital outcomes (highlighted in green in the figure) is possible through close planetary encounters; this can cause both asynchronous

Table 5
Origin of Spin-Orbital Properties

System	a/R_p	e	Tides	BYORP	Flyby	Kozai
2000 DP107	6.6	0.01	Yes	Yes	No	No
1999 KW4	3.9	0.008	Yes	Yes	No	No
2002 CE26	2.8	0.025	Yes	Yes	No	No
*2004 DC	4.4	0.30	Yes	No	Yes	No
*2003 YT1	7.1	0.18	Yes	No	Yes	No
Didymos	3.0	0.04	Yes	Yes	No	No
*1991 VH	5.4	0.06	Yes	No	Yes	No
2001 SN263 #1	2.9	0.016	Yes	Yes	No	No
*2001 SN263 #2	13	0.015	Yes	No	No	No
1994 CC #1	5.6	0.002	Yes	Yes	No	No
*1994 CC #2	20	0.19	No	No	No	No

For each system’s satellite, we list the adopted values for the observed semi-major axis a/R_p and eccentricity e , as well as which evolutionary process(es) can explain its observed spin-orbital state. ‘Yes’ (in green) means that the considered process is plausible and we find no evidence to rule it out; the opposite response is ‘No,’ (in red) meaning the considered process is highly unlikely.

* Known asynchronous satellites

and synchronous rotators in circular orbits to evolve into asynchronous satellites with eccentric orbits, or any state into an asteroid pair or contact binary (shown by arrows with no starting point in the figure).

We now consider inward evolution from “synchronous and circular” and “asynchronous (chaotic) and eccentric” states. A synchronous satellite will be affected by BYORP and depending on its shape and rotation, can migrate inwards and become a contact binary. In the model of Čuk & Nesvorný (2010), a chaotically-spinning (and therefore asynchronous) satellite in an eccentric orbit will eventually temporarily regain synchronization with an orientation switched by 180 degrees, in which case BYORP would regain control of the system’s evolution and restore it to a stable state. Inward migration can follow and lead to the formation of a contact binary or, after sufficient inward migration, the effects of BYORP and tides can cancel, leading to a stable equilibrium (e.g. Jacobson & Scheeres 2011b) and a tidally-damped eccentricity. This would result in a synchronous satellite in a circular orbit.

We now consider outward evolution from the “synchronous and circular” and “asynchronous (chaotic) and eccentric” states. According to Čuk & Nesvorný (2010), outward migration leads to an increase in eccentricity, so a synchronous and circular state can become chaotically asynchronous and eccentric. Once chaotically asynchronous and eccentric, it would remain so unless the satellite can re-orient itself such that if synchronization is temporarily regained, BYORP can migrate the satellite inwards. According to McMahon & Scheeres (2010a,c), outward migration leads to a decrease in eccentricity, which means that synchronization will be maintained, aided in part by the restoring torque due to the satellite’s permanent deformation. In this model, outward migration would allow the “synchronous and circular” state to evolve into an asteroid pair.

Examples of NEA satellites in each spin-orbital state are also given in Figure 3. There are several examples of each end state, except for asynchronous satellites with

circular orbits and asteroid pairs. The only known example of an asynchronous satellite with a circular orbit is the outer satellite in triple 2001 SN263. Asynchronous and circular configurations may be rare because asynchronous satellites are more likely to be well-separated from their primary, and larger separations are more susceptible to stronger disruptive planetary encounters with short encounter timescales (Fang & Margot 2011). Strong and frequent planetary encounters can easily evolve asynchronous and circular configurations to asynchronous and eccentric states, making it more rare to observe an asynchronous and circular system.

As for asteroid pairs, none have been definitively reported in the near-Earth population although they have been observed in the main belt (i.e. Pravec et al. 2010). We briefly discuss implications for the formation of NEA asteroid pairs. Figure 3 shows how asteroid pairs can form directly through post-fission dynamics or planetary encounters. The BYORP model by McMahon & Scheeres (2010a,c) provides an additional route to their creation via BYORP-dominated expansion of a satellite’s orbit and the BYORP model by Čuk & Nesvorný (2010) does not predict this. Determination of likely asteroid pair formation mechanisms can elucidate which BYORP model (Čuk & Nesvorný (2010) or McMahon & Scheeres (2010a,c)) predicts the correct behavior. If BYORP-induced expansion of a binary’s mutual orbit is responsible for creating NEA asteroid pairs, then we should expect to observe a few binaries with very large separations unless they are efficiently disrupted by planetary flybys (see Section 3). Alternatively, Čuk & Nesvorný (2010) have hypothesized that asteroid pairs are the result of scattering among satellites in triple systems. Such scattering can occur if both satellites are or used to be synchronous and BYORP led them into convergent orbits, which would result in unstable orbits and scattering. Components would then collide or be ejected.

7. CONCLUSION

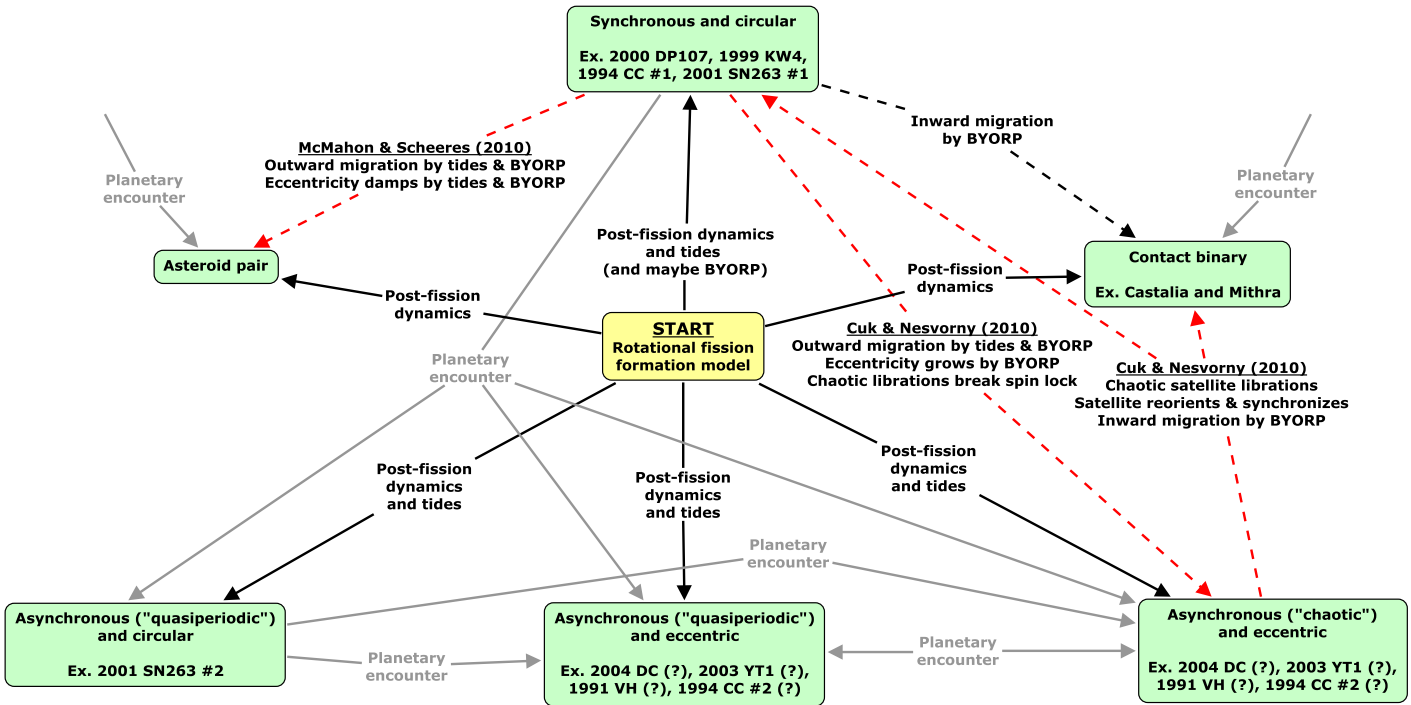


Figure 3. Possible spin-orbital pathways are shown for an evolving satellite in a newly post-fissioned NEA system with the assumption that Kozai oscillations are not relevant. Pathways that start and end in the same spin-orbital configuration are not shown in this figure, even though they may occur. Two different models are given for BYORP and are highlighted in red. Čuk & Nesvorný (2010) predict that BYORP-induced change in eccentricity has the same direction as the change in semi-major axis, and they model how a chaotically asynchronous satellite can reorient and regain synchronization. On the other hand, McMahon & Scheeres (2010a,c) predict that BYORP-induced change in eccentricity has a direction opposite of the change in semi-major axis. For synchronous and circular systems, it is possible that they are in the stable equilibrium of Jacobson & Scheeres (2011b). See Section 6 for additional discussion regarding this figure.

Radar observations of well-characterized NEA binaries and triples have uncovered a diverse set of spin-orbital properties: synchronous and asynchronously rotating satellites, circular and eccentric orbits, and a few large separations between the primary and the satellite. The formation of these satellites by rotational fission followed by a post-fission dynamics model (Jacobson & Scheeres 2011) can produce asynchronous satellites with a variety of primary separations and high orbital eccentricities. We investigated how a newly formed system can evolve to one of the observed systems by evaluating these evolutionary processes: tides, BYORP, planetary encounters, and Kozai effects.

We found that post-fission dynamics and tides can explain the observed semi-major axes, eccentricities, and satellite spin states of nearly all binaries and triples in our sample. Other evolutionary mechanisms do not appear to be dominant processes: BYORP is not applicable to asynchronous systems and is not required to explain the observed data, even though it may be acting; planetary encounters are likely not responsible for creating synchronous and circular configurations; and the Kozai effect will typically be suppressed by the primary’s oblateness.

We also illustrated the evolutionary pathways for satellites in binaries and triples after they have formed. Evolutionary processes such as tides, planetary encounters, and BYORP can evolve a system between syn-

chronous and circular, asynchronous and circular, and asynchronous and eccentric configurations.

We thank Peter Goldreich, Bill Bottke, Matija Čuk, and Shantanu Naidu for useful discussions, Seth Jacobson for providing the results from his post-fission dynamics simulations, and Jay McMahon for sending us a copy of his thesis. We are also grateful to the reviewer for helpful comments. This work was partially supported by NASA Planetary Astronomy grant NNX09AQ68G.

REFERENCES

Benner, L. A. M., Margot, J. L., Nolan, M. C., Giorgini, J. D., Brozovic, M., Scheeres, D. J., Magri, C., & Ostro, S. J. 2010, in *Bulletin of the American Astronomical Society*, Vol. 42, AAS/Division for Planetary Sciences Meeting Abstracts #42, 1056+
 Benner, L. A. M., Nolan, M. C., Margot, J. L., Ostro, S. J., & Giorgini, J. D. 2003, in *Bulletin of the American Astronomical Society*, Vol. 35, AAS/Division for Planetary Sciences Meeting Abstracts #35, 959+
 Bottke, W. F., Durda, D. D., Nesvorný, D., Jedicke, R., Morbidelli, A., Vokrouhlický, D., & Levison, H. F. 2005, *Icarus*, 179, 63
 Bottke, W. F., Morbidelli, A., Jedicke, R., Petit, J.-M., Levison, H. F., Michel, P., & Metcalfe, T. S. 2002, *Icarus*, 156, 399

- Brozovic, M., Benner, L. A., Taylor, P. A., Nolan, M. C., Howell, E. S., Magri, C., Scheeres, D. J., Giorgini, J. D., Pollock, J. T., Pravec, P., Gald, A., Fang, J., Margot, J.-L., Busch, M. W., Shepard, M. K., Reichart, D. E., Ivarsen, K. M., Haislip, J. B., LaCluyze, A. P., Jao, J., Slade, M. A., Lawrence, K. J., & Hicks, M. D. 2011, *Icarus*, 216, 241
- Cash, W. 1976, *A&A*, 52, 307
- Čuk, M. 2007, *ApJ*, 659, L57
- Čuk, M. & Burns, J. A. 2005, *Icarus*, 176, 418
- Čuk, M. & Nesvorný, D. 2010, *Icarus*, 207, 732
- Fang, J., Margot, J., Brozovic, M., Nolan, M. C., Benner, L. A. M., & Taylor, P. A. 2011, *AJ*, 141, 154
- Fang, J. & Margot, J. L. 2011, *AJ*
- Goldreich, P. 1963, *MNRAS*, 126, 257
- Goldreich, P. & Sari, R. 2009, *ApJ*, 691, 54
- Harris, A. W., Fahnestock, E. G., & Pravec, P. 2009, *Icarus*, 199, 310
- Holsapple, K. A. 2010, *Icarus*, 205, 430
- Hudson, R. S. & Ostro, S. J. 1999, *Icarus*, 140, 369
- Jacobson, S. A. & Scheeres, D. J. 2011, *Icarus*
- Jacobson, S. A. & Scheeres, D. J. 2011a, in *Bulletin of the American Astronomical Society*, Vol. 43, AAS/Division for Planetary Sciences Meeting Abstracts #43
- Jacobson, S. A. & Scheeres, D. J. 2011b, *ApJ*, 736, L19+
- Kiseleva, L. G., Eggleton, P. P., & Mikkola, S. 1998, *MNRAS*, 300, 292
- Kozai, Y. 1962, *AJ*, 67, 591
- Lowry, S. C., Fitzsimmons, A., Pravec, P., Vokrouhlický, D., Boehnhardt, H., Taylor, P. A., Margot, J. L., Galád, A., Irwin, M., Irwin, J., & Kusnirák, P. 2007, *Science*, 316, 272
- Margot, J., Taylor, P. A., Nolan, M. C., Howell, E. S., Ostro, S. J., Benner, L. A. M., Giorgini, J. D., Magri, C., & Carter, L. M. 2008, in *Bulletin of the American Astronomical Society*, Vol. 40, AAS/Division for Planetary Sciences Meeting Abstracts #40, 433+
- Margot, J. L. & Brown, M. E. 2003, *Science*, 300, 1939
- Margot, J. L., Nolan, M. C., Benner, L. A. M., Ostro, S. J., Jurgens, R. F., Giorgini, J. D., Slade, M. A., & Campbell, D. B. 2002, *Science*, 296, 1445
- McMahon, J. & Scheeres, D. 2010a, *Icarus*, 209, 494
- McMahon, J. & Scheeres, D. 2010b, in *Bulletin of the American Astronomical Society*, Vol. 42, AAS/Division for Planetary Sciences Meeting Abstracts #42, 1093+
- . 2010c, *Celestial Mechanics and Dynamical Astronomy*, 106, 261
- Merline, W. J., Weidenschilling, S. J., Durda, D. D., Margot, J. L., Pravec, P., & Storrs, A. D. 2002, *Asteroids III*, 289
- Murray, C. D. & Dermott, S. F. 1999, *Solar system dynamics*
- Nicholson, P. D., Cuk, M., Sheppard, S. S., Nesvorný, D., & Johnson, T. V. 2008, *Irregular Satellites of the Giant Planets*, ed. Barucci, M. A., Boehnhardt, H., Cruikshank, D. P., Morbidelli, A., & Dotson, R., 411–424
- Nolan, M. C., Howell, E. S., Becker, T. M., Magri, C., Giorgini, J. D., & Margot, J. L. 2008, in *Bulletin of the American Astronomical Society*, Vol. 40, AAS/Division for Planetary Sciences Meeting Abstracts #40, 432+
- Nolan, M. C., Howell, E. S., & Miranda, G. 2004, in *Bulletin of the American Astronomical Society*, Vol. 36, AAS/Division for Planetary Sciences Meeting Abstracts #36, 1132+
- Ostro, S. J., Rosema, K. D., Hudson, R. S., Jurgens, R. F., Giorgini, J. D., Winkler, R., Yeomans, D. K., Choate, D., Rose, R., Slade, M. A., Howard, S. D., & Mitchell, D. L. 1995, *Nature*, 375, 474
- Ostro, S. J. et al. 2006, *Science*, 314, 1276
- Perets, H. B. & Naoz, S. 2009, *ApJ*, 699, L17
- Pravec, P. & Harris, A. W. 2007, *Icarus*, 190, 250
- Pravec, P., Harris, A. W., & Michalowski, M. 2002, in *Asteroids III*, ed. W. F. Bottke, A. Cellino, P. Paolicchi, & R. P. Binzel (Univ. of Arizona Press), 113–122
- Pravec, P., Vokrouhlický, D., Polishook, D., Scheeres, D. J., Harris, A. W., Galád, A., Vaduvescu, O., Pozo, F., Barr, A., Longa, P., Vachier, F., Colas, F., Pray, D. P., Pollock, J., Reichart, D., Ivarsen, K., Haislip, J., Lacluyze, A., Kušnirák, P., Henych, T., Marchis, F., Macomber, B., Jacobson, S. A., Krugly, Y. N., Sergeev, A. V., & Leroy, A. 2010, *Nature*, 466, 1085
- Pravec, P. et al. 2006, *Icarus*, 181, 63
- Press, W. H., Teukolsky, S. A., Vetterling, W. T., & Flannery, B. P. 1992, *Numerical recipes in C. The art of scientific computing*, ed. Press, W. H., Teukolsky, S. A., Vetterling, W. T., & Flannery, B. P.
- Rubincam, D. P. 2000, *Icarus*, 148, 2
- Scheeres, D. J. 2007, *Icarus*, 189, 370
- Scheeres, D. J., Marzari, F., & Rossi, A. 2004, *Icarus*, 170, 312
- Scheeres, D. J., Ostro, S. J., Werner, R. A., Asphaug, E., & Hudson, R. S. 2000, *Icarus*, 147, 106
- Shepard, M. K. et al. 2006, *Icarus*, 184, 198
- Sitarski, G. 1968, *Acta Astron.*, 18, 171
- Steinberg, E. & Sari, R. 2011, *AJ*, 141, 55
- Taylor, P. A. & Margot, J. L. 2011, *Icarus*, 212, 661
- Taylor, P. A., Margot, J. L., Nolan, M. C., Benner, L. A. M., Ostro, S. J., Giorgini, J. D., & Magri, C. 2008, *LPI Contributions*, 1405, 8322
- Taylor, P. A., Margot, J. L., Vokrouhlický, D., Scheeres, D. J., Pravec, P., Lowry, S. C., Fitzsimmons, A., Nolan, M. C., Ostro, S. J., Benner, L. A. M., Giorgini, J. D., & Magri, C. 2007, *Science*, 316, 274
- Walsh, K. J., Richardson, D. C., & Michel, P. 2008, *Nature*, 454, 188
- Williams, J. G., Boggs, D. H., & Ratcliff, J. T. 2008, in *Lunar and Planetary Institute Science Conference Abstracts*, Vol. 39, Lunar and Planetary Institute Science Conference Abstracts, 1484+
- Wisdom, J., Peale, S. J., & Mignard, F. 1984, *Icarus*, 58, 137